

Effect of local strain on single acceptors in Si

L. E. Calvet,^{1,2,*} R. G. Wheeler,² and M. A. Reed²

¹*Institut d'Electronique Fondamentale, Université Paris-Sud, UMR 8622 CNRS, Bâtiment 220, 91405 Orsay, France*

²*Department of Applied Physics and Department of Electrical Engineering, Yale University, New Haven, Connecticut 06520, USA*

(Received 29 January 2007; revised manuscript received 25 May 2007; published 16 July 2007)

We explore the low temperature transport through a resonant acceptor impurity located near a metal-semiconductor interface and observe a large shift (12 meV) and splitting (0.8 meV) of its ground state. The shift is attributed to the quadratic Stark effect resulting from the electric field of the electrostatic barrier. The splitting is too large to be attributed to a linear Stark splitting. We calculate the strain field due to a nearby point defect and show that it can cause a large ground state splitting.

DOI: [10.1103/PhysRevB.76.035319](https://doi.org/10.1103/PhysRevB.76.035319)

PACS number(s): 73.30.+y, 73.40.Gk, 71.55.Cn

I. INTRODUCTION

The electronic spectra of shallow donors and acceptors in silicon have been investigated extensively in samples containing many impurities.¹ The majority of this research was conducted over 30 years ago and was important for realizing semiconductor devices, most notably transistors, where charges on impurities are used to modulate current transport. Transistors made small enough can be greatly influenced by the inhomogeneous nature of doping²⁻⁴ and thus understanding variations in the spectra of single impurities is of great interest. While investigations of randomly positioned single dopants have a long history,⁵⁻⁸ recent research has demonstrated unprecedented transport spectroscopy of single impurities.^{4,9} In this paper, we draw on results from bulk experiments¹⁰ to understand the spectra of single acceptor impurities in silicon. These results are interesting for those working on ultrasmall transistors and the realization of qubits based on single dopants,¹¹⁻¹⁶ where the environmental influence of nearby metallic contacts can strongly affect spin and charge relaxation and decoherence.¹⁷

An ongoing subject in spectroscopy of bulk samples is understanding the linewidths and line shapes of the spectra.¹⁰ This topic has been particularly important for shallow acceptors such as boron, where electron paramagnetic resonance was initially unsuccessful.¹⁸ Such dopants are fourfold degenerate and the presence of random strains or electric fields can result in a distribution of doublet splittings that can broaden the EPR transitions rendering them unobservable. Feher *et al.* were able to overcome this by applying a sufficiently large external strain.¹⁹ Later, Neubrand showed that high quality dislocation-free silicon permitted observation of the A^0 ground state of a shallow boron acceptor without external applied strain.²⁰ This research, however, also reported a sample-independent distribution of “intrinsic” A^0 splittings²¹ that were subsequently the subject of much research and have been attributed to (1) a large concentration of interstitial silicon point defects,²¹ (2) a lowering of the A^0 symmetry by a dynamic Jahn-Teller effect,^{22,23} and (3) most recently quite convincingly isotopic effects.^{24,25}

Here, we consider single confined acceptors located in the metal/semiconductor contact or Schottky barrier of a Schottky barrier metal-oxide-semiconductor field effect transistor (SBMOSFET), depicted in the insets of Fig. 1. The

splitting seen here (0.8 meV) is much larger than the intrinsic splitting observed in bulk samples (0.01 meV), and is most likely a result of our device geometry. We use the models developed to describe strain due to interstitial point defects to understand our experiment.

II. EXPERIMENTAL METHODS

The SBMOSFET is different from a conventional MOSFET in that the source and drain consist of the metallic alloy PtSi instead of the traditional p - n junctions. While SBMOSFETs are candidates for nanoscale Si devices,²⁶ they also provide a convenient tool to investigate the energy spectrum of dopants.⁹ Specifically, at low temperatures and small source-drain voltages, electron transport is governed by direct tunneling through the Schottky barriers (SBs).²⁷ If a randomly situated impurity is located near the metal/semiconductor interface, its transport will be superimposed on the direct tunneling current and easily observable in the transport, as shown in Fig. 1(a). Even though impurities near the SB are at approximately the same value in energy relative to the valence band (Ry^*), their absolute position in energy varies with their distance from the metallic contact (x axis) and their position relative to the MOS surface (z axis). For a sufficiently dilute doping concentration and small device geometry, we find individual resonances that are well separated in V_g .

The structure utilized in these investigations is a device consisting of an n -type polysilicon gate, a boron doped substrate ($n=5 \times 10^{21} \text{ m}^{-3}$), and a 34 Å gate oxide.^{27,28} The source and drain were made from depositing 300 Å of Pt and annealing to form the metallic alloy PtSi. The number of observed resonances scaled with the physical device width; thus, choosing a sufficiently dilute impurity system ensures that individual impurities are well separated for spectroscopy. We have observed typically ~ 6 – 7 resonances for 20 μm width devices, ~ 3 for 10 μm widths, and 1 or 2 for 5 μm widths. Here, we consider a 20 μm width device. Throughout this paper, we assume that the effects of the electric and magnetic fields are a small perturbation on the properties of the impurity.

$I(V_g)$ measurements were taken in He-4 cryostat at 1.5 and at 4 K in the insert of a 9 T magnet. The direction of

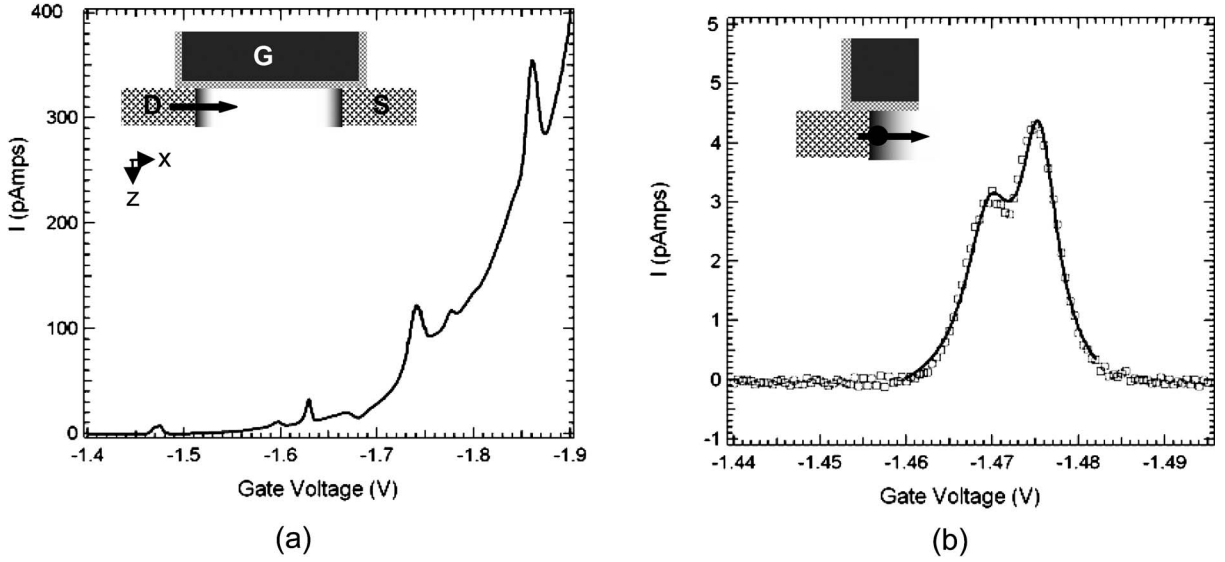


FIG. 1. (a) $I(V_g)$ characteristics of the device at 1.5 K $V_{ds}=0.5$ mV, showing the resonant peaks due to single impurities superimposed on the direct tunneling current through the entire Schottky barrier. The inset is a schematic of the device. S , D , and G signify the source, drain, and gate. A contour plot of the depletion potential is drawn near the source/drain, where black is ~ 0.2 eV and white is 0 eV relative to the valence band. (b) $I(V_g)$ characteristics of the impurity at 1.5 K and $V_{ds}=0.2$ mV. Note that at this small gate bias, the direct tunneling current is negligible. The dotted lines are the data and the solid line is a fit to the Landauer equation. The inset depicts the position of the impurity near the semiconductor/metallic interface.

transport was in $[110]$ and the magnetic field was applied perpendicular to the two-dimensional hole gas in the $[001]$ direction. This is the same device as in Ref. 9, but we investigate a different impurity, located at a different V_g .

III. STARK EFFECT

The ground state splitting $2\Delta=0.8$ meV at 1.5 K is shown in Fig. 1(b). The impurity is subject to an electric field due to the built-in potential of the Schottky barrier and can potentially exhibit a Stark effect. The SB exerts an electric field E along the transport direction; thus, the ground state can experience both a linear splitting and a quadratic shift: $\Delta = \pm \Delta_E + \Delta_{E^2}$, where Δ_E is the linear splitting and $\Delta_{E^2}=a_8 E^2$ is the quadratic shift associated with the quadratic dipole moment a_8 of the Γ_8 level.^{29,30} The linear effect is too small to be observed at this temperature^{9,31} and we concentrate on the quadratic term.

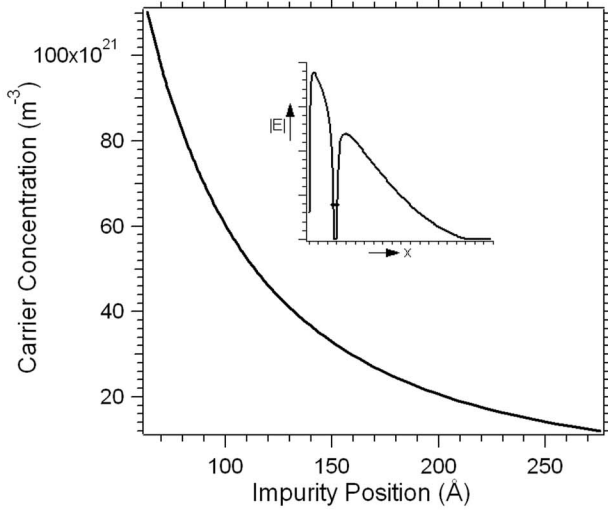
The total potential of the Schottky barrier and hydrogenic impurity can be modeled using a standard metal-semiconductor contact and hydrogenic potential, as shown in the inset of Fig. 2(a). We consider the energy of the resonant impurity, situated at $x=a$, the distance of the impurity from the metal/semiconductor interface:

$$V(a) = -\frac{qn_s}{\epsilon_s} \left(wa - \frac{a^2}{2} \right) + \phi_{ib} - \frac{q}{16\pi\epsilon_s a} - Ry^* - \Delta_{E^2}.$$

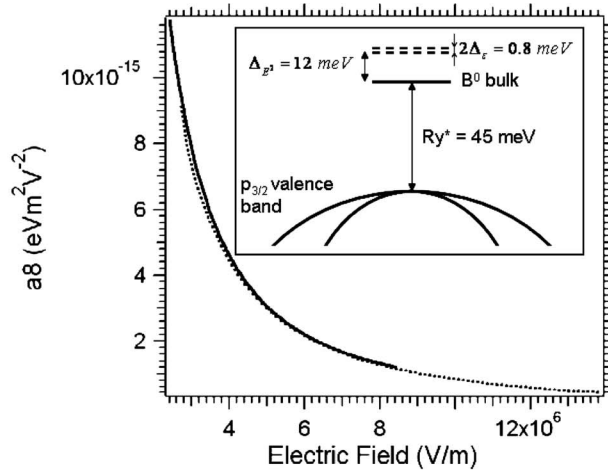
The first three components of this equation are the standard metal-semiconductor depletion approximation with image charge where n_s is the effective carrier concentration at a

distance z from the oxide surface and $\phi_{ib}=0.225$ eV is the intrinsic Schottky barrier height. $Ry^*=0.045$ eV is the effective Rydberg for a boron impurity in silicon. The last two terms represent the position of the resonance level relative to the valence band. To determine Δ_{E^2} one must first determine n_s and a . Following the method reported previously,⁹ we determine a range of possible n_s corresponding to a unique a . The resulting fitting parameters used to determine this range are given in Table I and the values of n_s are shown in Fig. 2(a). Using the expression for $V(a)$, we find $\Delta_{E^2} \sim 12 \pm 0.01$ meV for this impurity, which is similar to that found in the impurity considered in previous work,⁹ $\Delta_{E^2} \sim 12 \pm 0.008$ meV. Note that this shift represents an energetic position that is deeper in the silicon band gap.

It is striking that the quadratic Stark shift is so similar in these two impurities when their resonant energy levels differ by 22.5 meV. This is a strong indication that the electric field felt by each impurity is very similar. It may be that the transmission coefficients of the impurities in the Schottky barrier limit the observation of single impurities to a small region along the x and z axes. The values for a_8 are reported in Fig. 2(b). As shown in the inset of Fig. 2(b), these shifts are 2 orders of magnitude larger than the linear Stark effect (~ 0.1 meV) and an order of magnitude larger than the ground state splitting observed here (~ 0.8 meV). There is one report of the quadratic dipole moments for boron in the literature.³² This early work assumed that the ground state shift was negligible compared with the excited shifts. Our results indicate that the ground state shift can be large, as our range of a_8 is comparable to their reported values for the excited state quadratic dipole moments.



(a)



(b)

FIG. 2. (a) Carrier concentration n_s versus impurity position. These values were obtained using the ratio of the fitted leak rates from Table I WKB approximation (Ref. 9). The inset shows the total potential of an impurity located at 14 nm from the metal with $n_s = 3 \times 10^{22} \text{ m}^{-3}$. (b) The quadratic dipole moment a_8 for the impurity in the main text (solid line) and that from Ref. 9 (dotted line) vs electric field. The inset shows the relative values of Ry^* , Δ_E^2 , and Δ_E . Note that Δ_E is too small to be put in this schematic.

IV. MAGNETIC FIELD

In an applied magnetic field, there are two additional contributions to the Hamiltonian: a diamagnetic term given by $e^2 B^2 r^2 / 8m^*$ and a Zeeman splitting. The diamagnetic effect is observed when the magnetic field significantly alters the overlap between the impurity and the electrodes:⁶ $e^2 B^2 r^2 / 8m^* \approx e^2 / 4\pi\epsilon_s r$, where r is the overlap distance. As field is increased, the wave function is compressed and thus in addition to the diamagnetic shift cited above, a significant change in the leak rates occurs. In the presence of asymmet-

TABLE I. Parameters used to obtain n_s , shown in Fig. 2(a). V_{gres}^0 and Δ are obtained directly from the data and the leak rates from the fit to the Landauer equation (Ref. 9).

V_{gres}^0 (V)	2Δ (mV)	Γ_L^+ (10^{-3} V)	Γ_L^- (10^{-3} V)	Γ_R^+ (10^{-4} V)	Γ_R^- (10^{-4} V)
-1.4725	5.8	4.91 ± 0.14	6.64 ± 0.24	3.96 ± 0.11	3.57 ± 0.12

ric barriers as here, the smallest leak rate will be suppressed more rapidly than the larger one, resulting in a sharp attenuation of the peak height with field.

The Zeeman effect completely lifts the fourfold degeneracy of acceptor impurities and is thus a sensitive probe of the spectra. Acceptors in silicon have been studied both theoretically²⁹ and for B^0 in silicon experimentally.³³ With the magnetic field applied in [001], the Zeeman splittings in the absence of quadratic effects are described by $\Delta E_z = E_{m_j} - E_0 = g_{|m_j|} \mu_B m_j B$, where $m_j = +3/2, +1/2, -1/2$, and $-3/2$. We note that to first order the Zeeman splittings are independent of strain.¹⁹ Reported values of g range from 0.9 to 1.2 (Ref. 31). In previous research, the small ground state splitting due to the linear Stark effect was of the same order as the Zeeman energy. In this work, the ground state splitting is larger.

In Fig. 3(a), we show the magnetic field dependence of the split ground state of the device. With increasing field the positive peak is displaced to lower energy, while the negative peak becomes broader and increases in height. These two effects can be attributed to a Zeeman splitting and thus dominate any signatures of the diamagnetic term. The peak position versus magnetic field is shown in Fig. 3(b), where we have plotted the full width at half maximum Γ as error bars. We note that at 5 T, $\Gamma > 2\Delta$ and the significant mixing of the levels means that m_j is not a good quantum number. We thus fit between 2 and 5 T. For the $m_j = -1/2$ level, we find $g_{1/2} = 0.97 \pm 0.06$. Similarly, the change in the broadening of the lower level is attributed to the incomplete Zeeman splitting of the $m_j = \pm 3/2$ levels and a linear fit reveals $g_{3/2} = 1.26 \pm 0.08$. These values are consistent with boron impurities in bulk silicon³³ and with our previous results. We note that the difference in g factors cannot be due to a Jahn-Teller effect²² because one expects to observe an *increase* of the g factor when the orbital ground state is nondegenerate. In this paper, the Zeeman splitting is a perturbation on the ground state splitting ($g_{1/2} = 0.97$), whereas in previous work, the ground state orbital splitting was smaller than the Zeeman splitting ($g_{1/2} = 1.14$). The cause of the difference in the g factor observed in the two impurities is unclear. It may be a result of the anisotropy of the bands near the metal/semiconductor interface.

The combination of similar quadratic Stark shifts and Zeeman splittings provides strong evidence that the impurity investigated here and that in previous work⁹ are most likely the same species, despite the large difference in the ground state splitting.

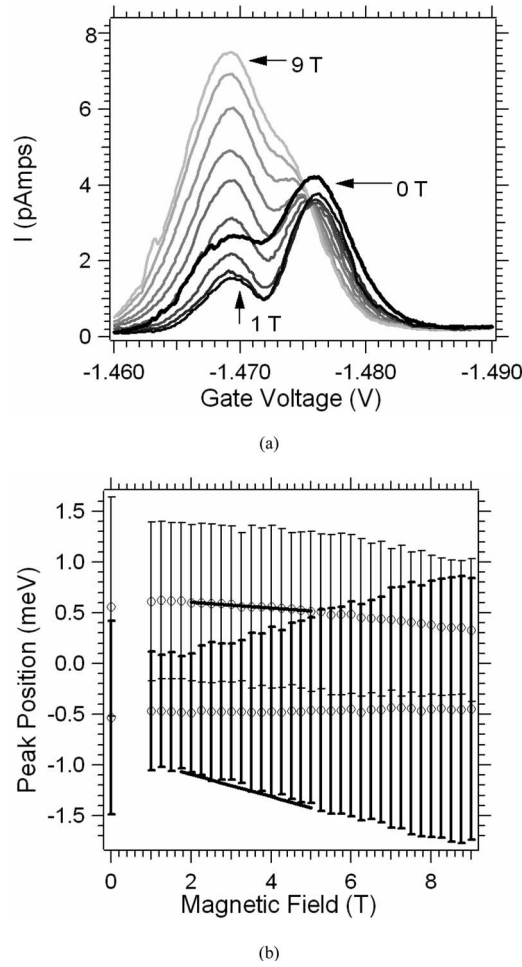


FIG. 3. (a) $I(V_g)$ as a function of magnetic field at 4 K and $V_{ds}=0.1$ mV, showing the data from 0 to 9 T in steps of 1 T. The 0 T curve is shown in a thick black line. (b) Fan diagram showing the peak positions as a function of magnetic field. Data were taken from 0 to 9 T in intervals of 0.25 T. The error bars indicate the full width at half maximum. The straight lines are linear fits from 2 to 5 T used to obtain the g factors.

V. MODEL: GROUND STATE SPLITTING DUE TO STRAIN FROM A SI SELF-INTERSTITIAL

Variations in the ground state splitting have been observed in impurity peaks in all of the five devices measured and are reminiscent of investigations of impurities in bulk semiconductors where inhomogeneously broadened resonant lines have been attributed to, among other effects,^{22–25} the presence of random strains or electric fields in the samples.^{10,18–21} Theoretical research shows that strain can add an additional splitting to that of an electric field.²⁹ Here, we consider the possibility that the observed large ground state splitting is the result of a nearby strain field. There are two possible origins: (1) strain due to the PtSi/Si interface and (2) local fields due to a nearby point defect.

Our measurements eliminate the first scenario. Previous work that investigated strain in bulk samples observed

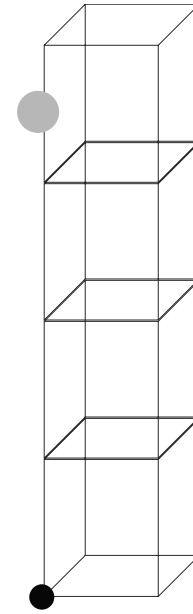


FIG. 4. Schematic of the cubic silicon lattice in the z direction, where silicon atoms are assumed to be at the corners of the cubes. The substitutional boron impurity, small black dot, is placed at the bottom left corner and the silicon interstitial responsible for the strain, large gray dot, is located at $7/2a_{lat}$.

that the g factor is anisotropic with respect to the angle θ between the stress axis and the magnetic field: $g^2 = g_{\perp}^2 \cos^2 \theta + g_{\parallel}^2 \sin^2 \theta$, where $g_{\perp} \approx 2g_{\parallel} \approx 2g_{1/2} = 2g_{3/2}$.¹⁹ Strain from the PtSi/Pt interface is perpendicular to the applied magnetic field and would thus result in much larger g factors.

We consider the possibility of a nearby point defect. Symmetry arguments and previous experimental research show that the ground state of boron under tensile stress should split into an upper level with $m_j = \pm 3/2$ and a lower level with $m_j = \pm 1/2$. Since we have exactly the opposite situation and because the magnetic field dependence indicates strain that is approximately parallel to its direction, we argue that the most likely point defect would be a self-interstitial located in the $[001]$ direction. Self-interstitials are highly probable in this device because (1) the formation of PtSi injects silicon interstitials into the silicon bulk³⁴ and (2) diffusion of boron takes place via a B-Si self-interstitial complex.³⁵

Building on previous research developed to describe the inhomogeneous broadening of the ESR spectrum of bulk impurities,^{10,21} we model the effect of a neighboring self-interstitial located close to the boron impurity. A point defect at a distance \mathbf{r} from the impurity in an isotropic continuum produces a displacement vector at the boron impurity of the form $\mathbf{u}(\mathbf{r}) = -A(\mathbf{r}/r^3)$, where $A \approx 0.8 \text{ \AA}^3$ (Ref. 21) is the “elastic strength” of the point defect. The components of the strain tensor are given by $\varepsilon_{ij} = \frac{1}{2}(\partial u_i / \partial x_j + \partial u_j / \partial x_i)$. The splitting of an impurity level due to strain $2\Delta_{\varepsilon}$ is²⁹

$$\Delta_\varepsilon = \pm \sqrt{\frac{b^2}{2}[(\varepsilon_{xx} - \varepsilon_{yy})^2 + (\varepsilon_{xx} - \varepsilon_{zz})^2 + (\varepsilon_{yy} - \varepsilon_{zz})^2] + d^2(\varepsilon_{xy}^2 + \varepsilon_{xz}^2 + \varepsilon_{yz}^2)},$$

where b and d are the constants of the deformation potential for boron. We use the values of $b = -1.9$ eV and $d = -4.84$ eV from experiments on bulk samples³⁶ and calculate the strain splitting for an interstitial located in the $[001]$ direction. We find that an interstitial located at $\mathbf{r} = \frac{7}{2}a_{lat}\hat{z}$, where $a_{lat} = 5.4$ Å, as depicted in Fig. 4, results in $2\Delta_\varepsilon = 0.9$ meV. The isotropic continuum approximation is not quite correct in silicon and overestimates the effect of the strain field. Following the approximations for an anisotropic continuum used in the work of Neubrand (Ref. 21), we find that an impurity located at $\mathbf{r} = \frac{5}{2}a_{lat}\hat{z}$ will result in a splitting of $2\Delta_\varepsilon = 0.86$ meV.

VI. CONCLUDING REMARKS

Quantum computing proposals based on single dopants may be susceptible to the large variations in the ground state energies observed in this work. The electric and magnetic fields^{14,15} used to manipulate these states may not be sufficient to overcome such phenomena. Proposals based on phosphorus donor atoms as qubits^{11,12,16} may be equally affected by nearby point defects because they are subject to similar diffusion mechanisms.³⁵ The effects of external strain due to P-self-interstitial complexes have been investigated in

bulk samples and can reduce the valley-orbit splitting by 33%, resulting in a 15% reduction of the hyperfine splitting.³⁷

In summary, we have demonstrated a large quadratic shift of a single acceptor impurity due to the built-in potential of a Schottky barrier and a large ground state splitting that is consistent with a strain field resulting from a nearby self-interstitial. Although the presence of the PtSi Schottky barrier enhances the likelihood of point defects in our experiment, this research shows that the local environment can have a strong influence on the energy spectrum of an acceptor. These results suggest that single impurities used for quantum computing architectures may need to be situated in a relatively point-defect-free lattice. An astute choice of the gate dielectric could control such effects because surface reactions can selectively perturb the equilibrium point defect concentration.³⁸

ACKNOWLEDGMENTS

It is a great pleasure to thank C. Wang, J. P. Snyder, and J. R. Tucker for devices and helpful discussions. L.E.C. thanks the French Ministry of Research and the Université Paris-Sud for financial support. This work was funded in part by DARPA.

*laurie.calvet@ief.u-psud.fr

¹A. Ramdas and S. Rodriguez, Rep. Prog. Phys. **44**, 1297 (1981).

²T. Shinada, S. Okamoto, T. Kobayashi, and I. Ohdomari, Nature (London) **437**, 1128 (2005).

³Y. Ono, K. Nishiguchi, A. Fujiwara, H. Yamaguchi, H. Inokawa, and Y. Takahashi, Appl. Phys. Lett. **90**, 102106 (2007).

⁴H. Sellier, G. P. Lansbergen, J. Caro, S. Rogge, N. Collaert, I. Ferain, M. Jurczak, and S. Biesemans, Phys. Rev. Lett. **97**, 206805 (2006).

⁵A. B. Fowler, G. L. Timp, J. J. Wainer, and R. A. Webb, Phys. Rev. Lett. **57**, 138 (1986).

⁶T. E. Kopley, P. L. McEuen, and R. G. Wheeler, Phys. Rev. Lett. **61**, 1654 (1988).

⁷M. W. Dellow, P. H. Beton, C. J. G. M. Langerak, T. J. Foster, P. C. Main, L. Eaves, M. Henini, S. P. Beaumont, and C. D. W. Wilkinson, Phys. Rev. Lett. **68**, 1754 (1992); J. W. Sakai, P. C. Main, N. Lascala, A. K. Geim, L. Eaves, and M. Henini, Appl. Phys. Lett. **64**, 2563 (1994).

⁸M. R. Deshpande, J. W. Sleight, M. A. Reed, R. G. Wheeler, and R. J. Matyi, Phys. Rev. Lett. **76**, 1328 (1996); M. R. Deshpande, J. W. Sleight, M. A. Reed, and R. G. Wheeler, Phys. Rev. B **62**, 8240 (2000).

⁹L. E. Calvet, R. G. Wheeler, and M. A. Reed, Phys. Rev. Lett. **98**, 096805 (2007).

¹⁰A. M. Stoneham, Rev. Mod. Phys. **41**, 82 (1969).

¹¹B. E. Kane, Nature (London) **393**, 133 (1998).

¹²R. Vrijen, E. Yablonovitch, K. Wang, H. W. Jiang, A. Balandin, V. Roychowdhury, T. Mor, D. DiVincenzo, Phys. Rev. A **62**, 012306 (2000).

¹³A. M. Stoneham, A. J. Fisher, and P. T. Greenland, J. Phys.: Condens. Matter **15**, L447 (2003).

¹⁴B. Golding and M. I. Dykman, e-print arXiv:cond-mat/0309147.

¹⁵B. A. Bernevig and S.-C. Zhang, Phys. Rev. B **71**, 035303 (2005).

¹⁶L. C. L. Hollenberg, A. S. Dzurak, C. Wellad, A. R. Hamilton, D. J. Reilly, G. J. Milburn, and R. G. Clark, Phys. Rev. B **69**, 113301 (2004).

¹⁷R. W. Keyes, Comput. Sci. Eng. **7**, 36 (2005).

¹⁸W. Kohn, Solid State Phys. **5**, 257 (1957).

¹⁹G. Feher, J. C. Hensel, and E. A. Gere, Phys. Rev. Lett. **5**, 309 (1960).

²⁰H. Neubrand, Phys. Status Solidi B **86**, 269 (1978).

²¹H. Neubrand, Phys. Status Solidi B **90**, 301 (1978).

²²T. N. Morgan, Phys. Rev. Lett. **24**, 887 (1970).

²³V. A. Karasyuk, M. L. W. Thewalt, S. An, and E. C. Lightowers, Phys. Rev. Lett. **73**, 2340 (1994).

²⁴D. Karaiskaj, M. L. W. Thewalt, T. Ruf, M. Cardona, and M. Konuma, Phys. Rev. Lett. **89**, 016401 (2002).

- ²⁵D. Karaiskaj, G. Kirczenow, M. L. W. Thewalt, R. Buczko, and M. Cardona, *Phys. Rev. Lett.* **90**, 016404 (2003).
- ²⁶J. M. Larson and J. P. Snyder, *IEEE Trans. Electron Devices* **53**, 1048 (2006).
- ²⁷L. E. Calvet, R. G. Wheeler, and M. A. Reed, *Appl. Phys. Lett.* **80**, 1761 (2002).
- ²⁸C. Wang, J. P. Snyder, and J. R. Tucker, *Appl. Phys. Lett.* **74**, 1174 (1999).
- ²⁹G. L. Bir, E. I. Butikov, and G. E. Pikus, *J. Phys. Chem. Solids* **24**, 1467 (1963); **24**, 1475 (1963).
- ³⁰G. D. J. Smit, S. Rogge, J. Caro, and T. M. Klapwijk, *Phys. Rev. B* **70**, 035206 (2004).
- ³¹A. Köpf and K. Lassmann, *Phys. Rev. Lett.* **69**, 1580 (1992).
- ³²J. J. White, *Can. J. Phys.* **45**, 2695 (1967).
- ³³F. Merlet, B. Pajot, P. Arcas, and A. M. Jeanlouis, *Phys. Rev. B* **12**, 3297 (1975).
- ³⁴M. Wittmer and K. N. Tu, *Phys. Rev. B* **29**, 2010 (1984).
- ³⁵A. Ural, P. B. Griffin, and J. D. Plummer, *J. Appl. Phys.* **85**, 6440 (1999); B. Sadigh, T. J. Lenosky, S. K. Theiss, M.-J. Caturla, T. Diaz de la Rubia, and M. A. Foad, *Phys. Rev. Lett.* **83**, 4341 (1999).
- ³⁶H. R. Chandrasekhar, P. Fisher, A. K. Ramdas, and S. Rodrigues, *Phys. Rev. B* **8**, 3836 (1973).
- ³⁷O. Scheerer, U. Juda, and M. Höhne, *Phys. Rev. B* **57**, 9657 (1998).
- ³⁸P. M. Fahey, P. B. Griffin, and J. D. Plummer, *Rev. Mod. Phys.* **61**, 289 (1989).